Journal of Hazardous Materials 161 (2009) 102–110

Contents lists available at ScienceDirect

Journal of Hazardous Materials

journal homepage: www.elsevier.com/locate/jhazmat

Removal of direct blue-86 from aqueous solution by new activated carbon developed from orange peel

Ahmed El Nemr*, Ola Abdelwahab, Amany El-Sikaily, Azza Khaled

Department of Pollution, Environmental Division, National Institute of Oceanography and Fisheries, El-Anfoushy, Kayet Bey, Alexandria, Egypt

ARTICLE INFO

Article history:
Received 17 April 2007
Received in revised form 9 November 2007
Accepted 13 March 2008
Available online 21 March 2008

Keywords:
Orange peel
Activated carbon
Dye
Direct blue-86
Adsorption
Wastewater

ABSTRACT

The use of low-cost, easy obtained, high efficiency and eco-friendly adsorbents has been investigated as an ideal alternative to the current expensive methods of removing dyes from wastewater. This study investigates the potential use of activated carbon prepared from orange peel for the removal of direct blue-86 (DB-86) (Direct Fast Turquoise Blue GL) dye from simulated wastewater. The effects of different system variables, adsorbent dosage, initial dye concentration, pH and contact time were studied. The results showed that as the amount of the adsorbent increased, the percentage of dye removal increased accordingly. Optimum pH value for dye adsorption was determined as ~2.0. Maximum dye was sequestered within 30 min after the beginning for every experiment. The adsorption of direct blue-86 followed a pseudo-second-order rate equation and fit well Langmuir, Tempkin and Dubinin–Radushkevich (D–R) equations better than Freundlich and Redlich–Peterson equations. The maximum removal of direct blue-86 was obtained at pH 2 as 92% for adsorbent dose of 6 g L^{-1} and 100 mg L^{-1} initial dye concentration at room temperature. The maximum adsorption capacity obtained from Langmuir equation was 33.78 mg g^{-1}. Furthermore, adsorption kinetics of DB-86 was studied and the rate of adsorption was found to conform to pseudo-second-order kinetics with a good correlation ($R^2 > 0.99$) with intraparticle diffusion as one of the rate determining steps. Activated carbon developed from orange peel can be attractive options for dye removal from diluted industrial effluents since test reaction made on simulated dyeing wastewater show better removal percentage of DB-86.

1. Introduction

Effluent from the dyeing and finishing processes in the textile industry are known to contain highly colored species, high amounts of surfactant, dissolved solids and possibly harmful heavy metals such as Cr, Ni and Cu [1]. Highly colored wastes are not only aesthetically displeasing but also hinder light penetration and may in consequence disturb biological processes in water-bodies. Moreover, dyes itself are toxic to some organisms and hence disturb the ecosystem. In addition, the expanded uses of azo dyes have shown that some of them and their reaction products such as aromatic amines are highly carcinogenic [2,3], which make the removal of dyes before disposal of the wastewater is necessary. Many studies have been conducted on the toxicity of dyes and their impact on the ecosystem [4,5], as well as the environmental issues associated with the manufacture and subsequent usage of dyes [6,7].

Most of the used dyes are stable to photo-degradation, biodegradation and oxidizing agents [8]. Hence, investigations have been conducted on several physical or chemical methods of removing color from textile effluent. These studies include the use of coagulants [9], ultra-filtration [10], electro-chemical [11,12] and adsorption [13,14] techniques. The advantages and disadvantages of each technique have been extensively reviewed [15]. Among these methods, adsorption has been found to be an efficient and economic process to remove dyes, pigments and other colorants and also to control the bio-chemical oxygen demand [15]. Activated carbon (powdered or granular) is the most widely used adsorbent because it has excellent adsorption efficiency for organic compounds and heavy metals, but its use is somewhat limited due to its high cost which led to search for low-cost adsorbents or preparation of low-cost activated carbon.

Annual production of waste orange is estimated to be more than 1.0 million tons in Egypt. Accumulation of orange waste in the orange industries has resulted in two important problems which are land space occupation and pollution with phenolic compounds due to dumping of this waste. Since the orange peel is available free of cost from orange processing industries, only the carbonization of it is involved for the wastewater treatment. Hence, recycling of this solid waste for wastewater treatment would not only be economical but also will help to solve solid waste disposal problems.

* Corresponding author. Tel.: +20 35740944; fax: +20 35740944.
E-mail address: ahmedmoustafaelnemr@yahoo.com (A.E. Nemr).

0304-3894/$ – see front matter © 2008 Elsevier B.V. All rights reserved.
doi:10.1016/j.jhazmat.2008.03.060

Therefore the main objective of this study was to evaluate the possibility of using dried orange peel to develop a new low-cost activated carbon and study its application to remove direct blue-86 (DB-86), which is currently among the widely used commercial dyes in the printing of cotton and mucilage glue fabrics as well as, the dyeing of silk, wool and vinylon and there are only one recent published paper dealt with the removal of DB-86 [16]. Orange peel was previously investigated to adsorb Methyl orange, Methylene blue, Rhodamine B, Congo red, Methyl violet and Amido black [17,18] Acid Violet 17 [19], and Direct Red 23 and 80 [20,21]. Systematic evaluation of the parameters involved, such as pH, sorbents mass, initial dye concentration and time. The interference of the simulated wastewater on the adsorption of direct blue-86 was additionally investigated.

2. Materials and methods

2.1. Biomass

Orange peel was collected from a local fruit field in the north of Egypt and washed with tap water followed by washing with distilled water. After this, the clean orange peel biomass was oven dried at 105 °C for 96 h, and the dried orange peel was milled and sieved to select particles ≤0.500 mm for use [22].

2.2. Preparation of activated carbon from orange peel (COP)

The dried orange peel biomass 1.0 kg was added in small portion to 800 mL of 98% H_2SO_4 during 6 h and the resulting reaction mixture was kept overnight at room temperature followed by refluxing for 12 h in an efficient fume hood. After cooling to room temperature, the reaction mixture was poured onto cold water (3 L) and filtered. The resulting material was heated in an open oven at 150 °C for overnight followed by washing with 3 L distilled water and then soaked in 1% $NaHCO_3$ solution overnight to remove any remaining acid. The obtained carbon was then washed with distilled water until pH of the activated carbon reached 6, dried in an oven at 150 °C for 24 h in the absence of oxygen and sieved to the particle size ≤0.063 mm and kept in a glass bottle until used.

2.3. Preparation of synthetic solution

A stock solution of 1.0 g L^{-1} was prepared by dissolving the appropriate amount of direct blue-86 (Direct Fast Turquoise Blue GL; 97%; C.I. 74180, CAS no.: 1330-38-7; obtained from ISMA Dye Company, Kafr-El-Dawar, Egypt) in 100 mL and completed to 1000 mL with distilled water. Fig. 1 displays the structure of the direct blue-86 (DB-86), Chemical formula $C_{32}H_{14}O_6N_8S_2CuNa_2$. Different concentrations ranged between 5 and 100 mg L^{-1} of DB 86 were prepared from the stock solution and used to have the standard curve. All the chemicals used throughout this study were of analytical-grade reagents. Double-distilled water was used for preparing all of the solutions and reagents. The initial pH is adjusted with 0.1 M HCl or 0.1 M NaOH. All the adsorption experiments were carried out at room temperature (25 ± 2 °C).

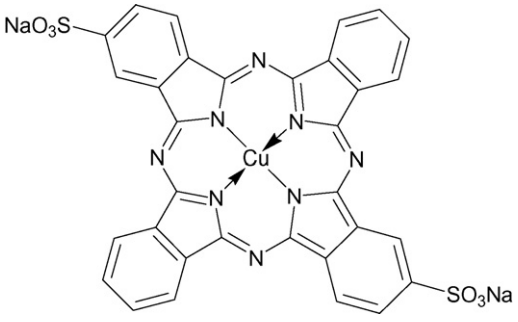

Fig. 1. Structure of direct blue-86 (Direct Fast Turquoise Blue GL), M. wt. = 778.96.

2.4. Batch biosorption studies

2.4.1. Effect of pH on DB-86 biosorption

The effect of pH on the equilibrium uptake of dye was investigated by employing initial concentration of DB-86 (100 mg L^{-1}) and 6 g L^{-1} of COP. The initial pH values were adjusted with 0.1 M HCl or 0.1 M NaOH to form a series of pH from 1 to 9. The suspensions were shaken at room temperature (25 ± 2 °C) using agitation speed (200 rpm) for the minimum contact time required to reach the equilibrium (180 min) and the amount of DB-86 adsorbed determined.

2.4.2. Effect of COP dose

The effect of sorbents dose on the equilibrium uptake of DB-86 (25, 50, 75, 100 and 125 mg L^{-1}) was investigated with COP concentrations of 2, 4 and 6 g L^{-1}. The experiments were performed by shaking known DB-86 concentration with the above different COP concentrations to the equilibrium uptake (180 min) and the amount of DB-86 adsorbed determined.

2.4.3. Kinetics studies

Sorption studies were conducted in 250-mL conical flasks at solution pH 2.0. COP (2, 4, and 6 g L^{-1}) was thoroughly mixed individually with 100 mL of DB-86 solution (25, 50, 75, 100, and 125 mg L^{-1}) and the suspensions were shaken at room temperature. Samples of 1.0 mL were collected from the duplicate flasks at required time intervals viz. 5, 10, 20, 30, 45, 60, 90, 120, 150 and 180 min and were centrifuged for 5 min. The clear solutions were analyzed for residual DB-86 concentration in the solution.

2.4.4. Adsorption isotherm

Batch sorption experiments were carried out in 250-mL conical flasks at room temperature on a shaker for 180 min. The COP (0.2, 0.4 and 0.6 g) was thoroughly mixed with 100 mL of DB-86 solutions. The isotherm studies were performed by varying the initial DB-86 concentrations from 25 to 125 mg L^{-1} at pH 2.0, which was adjusted using 0.1 M HCl or 0.1 M NaOH before addition of COP and maintained throughout the experiment. After shaking the flasks for 180 min, the reaction mixture was analyzed for the residual DB-86 concentration.

The concentration of DB-86 in solution was measured by using a direct UV–vis spectrophotometeric method using UV–vis spectrophotometer (Milton Roy, Spectronic 21D) using silica cells of path length 1 cm at wavelength λ 594 nm, and DB-86 concentration was determined by comparing absorbance to a calibration curve mentioned above. All the experiments are duplicated and only the mean values are reported. The maximum deviation observed was less than ±4%.

Adsorption of DB-86 from simulated wastewater was studied using 6 g L^{-1} of COP and DB-86 concentrations 100 mg L^{-1} at initial pH 2.0. The amount of dye adsorbed at equilibrium onto carbon, q_e (mg g^{-1}), was calculated by the following mass balance relationship:

$$q_e = (C_0 - C_e) \times \frac{V}{W} \quad (1)$$

where C_0 and C_e are the initial and equilibrium liquid-phase concentrations of DB-86, respectively (mg L^{-1}), V the volume of the solution (L), and W is the weight of the COP used (g).

3. Results and discussion

3.1. Effect of system pH on DB-86 uptake

The pH of the system exerts profound influence on the adsorptive uptake of adsorbate molecule presumably due to its influence on the surface properties of the adsorbent and ionization/dissociation of the adsorbate molecule. Fig. 2 shows the variations in the removal of dye from wastewater at various system pH. From the figure, it is evident that the maximum removal of DB-86 color is observed at pH 2. Similar trend of pH effect was observed for the adsorption of Direct Red 28 and Acid Violet on activated carbon prepared from coir pith [23,24], as well as for the adsorption of direct blue 2B and Direct Green B on activated carbon prepared from Mahogany sawdust [25]. That may be attributed to the hydrophobic nature of the developed carbon which led to absorb hydrogen ions (H^+) onto the surface of the carbon when immersed in water and make it positively charged. Low pH value (1.0–3.0) leads to an increase in H^+ ion concentration in the system and the surface of the activated carbon acquires positive charge by absorbing H^+ ions. As the COP surface is positively charged at low pH value, a significantly strong electrostatic attraction appears between the positively charged carbon surface and anionic dye molecule leading to maximum adsorption of DB-86. On the other hand, increase of the pH value (basic condition) led to increase of the number of negatively charged sites and the number of positively charged sites decreases. A negatively charged surface site on the COP dose not favor the adsorption of anionic DB-86 molecules due to the electrostatic repulsion. The lowest adsorption occurred at pH 8.0 and the greatest adsorption occurred at pH ~ 2.0. Sorbents surface would be positively charged up to pH < 4, and heterogeneous in the pH range 4–6. Thereafter, it should be negatively charged. Moreover, the decreasing in the adsorption of DB-86 with increasing of pH value is also due to the competition between anionic dye and excess OH^- ions in the solution. At pH value > 8 a small precipitation of DB-86 was observed, which explain the small increase in the dye removal at pH 9.

3.2. Effect of contact time and initial DB-86 concentration

The relation between removal of DB-86 and reaction time were studied to see the rate of dye removal. The results of percentage removal of DB-86 at pH 2.0 with increasing of contact time using COP are presented in Fig. 3. It was found that more than 64% removal of DB-86 concentration occurred in the first 5 min, and thereafter the rate of adsorption of the DB-86 onto COP was found to be slow. The rapid adsorption at the initial contact time is due to the availability of the positively charged surface of the COP for adsorption of anionic DB-86 in the solution at pH 2. The later slow rate of DB-86 adsorption is probably occurred due to the electrostatic hindrance or repulsion between the adsorbed negatively charged sorbate species onto the surface of COP and the available anionic sorbate species in solution as well as the slow pore diffusion of the solute ions into the bulk of the adsorbent. The equilibrium was found to be nearly 180 min when the maximum DB-86 adsorption onto COP was reached.

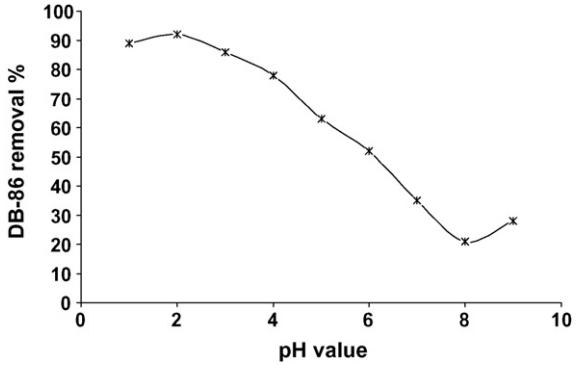

Fig. 2. Effect of system pH on adsorption of DB-86 (100 mg L^{-1}) onto COP (6 g L^{-1}) at room temperature (25 ± 2 °C), agitation speed 200 rpm for the minimum contact time required to reach the equilibrium (180 min).

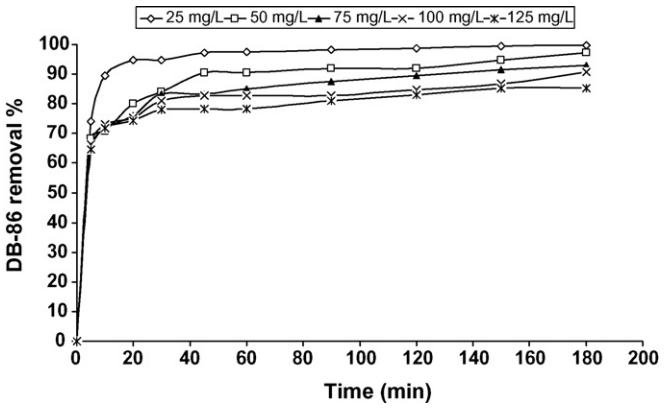

Fig. 3. Effect of contact time on the removal of different initial concentrations of DB-86 using COP (6 g L^{-1}) at pH 2.0.

Also, the effect of initial concentration of DB-86 in the solution on the capacity of adsorption onto COP was studied and shown in Fig. 3. The experiments were carried out at fixed adsorbent dose (0.6 g/100 mL) in the test solution, room temperature (25 ± 2 °C), pH 2 and at different initial concentrations of DB-86 (25, 50, 75, 100 and 125 mg L^{-1}) for different time intervals (5, 10, 20, 30, 45, 60, 90, 120, 150 and 180 min). Fig. 3 showed that the percentage of adsorption efficiency of COP decreased with the increasing of initial DB-86 concentration in the solution. Though the percent adsorption decreased with increase in initial dye concentration, the actual amount of DB-86 adsorbed per unit mass of adsorbent increased with increase in DB-86 concentration in the test solution.

It is evident from Fig. 3 that the amount adsorbed on the solid phase COP at a lower initial concentration of DB-86 was smaller than the corresponding amount when higher initial concentrations were used. However, the percentage removal of DB-86 was greater at lower initial concentrations and smaller at higher initial concentrations. The adsorption capacity for COP was increased from 10.84 to 39.98 mg g^{-1} as the DB-86 concentration increased from 25 to 125 mg L^{-1}. In the process of DB-86 adsorption initially dye molecules have to first encounter the boundary layer effect and then it has to diffuse from boundary layer film onto adsorbent surface and then finally, it has to diffuse into the porous structure of the adsorbent. This phenomenon will take relatively longer contact time.

3.3. Effect of adsorbent mass on DB-86 adsorption

The adsorption of DB-86 on COP was studied by changing the quantity of adsorbent (0.2, 0.4, 0.6, 0.8 and 1.0 g/100 mL) in the test solution while keeping the initial DB-86 concentration (125 mg L^{-1}), temperature (25 ± 2 °C) and pH (2.0) constant at contact times for 180 min (Fig. 4). The adsorption increased from 64% to 100%, as the COP dose increased from 0.2 g to 1.0 g/100 mL at equilibrium time (180 min). Maximum DB-86 removal was achieved within 10–25 min after which DB-86 concentration in the reac-

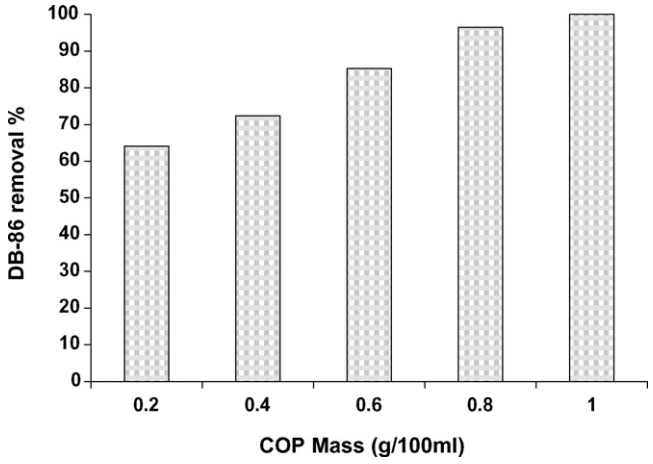

Fig. 4. Effect of adsorbent concentration on DB-86 removals (C_0: 125 mg L^{-1}, pH 2.0, agitation speed: 200 rpm, temperature: 25 ± 2 °C).

tion solution was almost constant. Increase in the adsorption with adsorbent dose can be attributed to increased COP surface area and availability of more adsorption sites, while the unit adsorbed of DB-86 decreased with increase in COP dose.

3.4. Isotherm data analysis

The relationship between the amount of a substance adsorbed at constant temperature and its concentration in the equilibrium solution is called the adsorption isotherm. The adsorption isotherm is important from both a theoretical and a practical point of view. In order to optimize the design of an adsorption system to remove the dye, it is important to establish the most appropriate correlations of the equilibrium data of each system. Equilibrium isotherm equations are used to describe the experimental sorption data. The parameters obtained from the different models provide important information on the sorption mechanisms and the surface properties and affinities of the sorbent. The most widely accepted surface adsorption models for single-solute systems are the Langmuir and Freundlich models. The correlation with the amount of adsorption and the liquid-phase concentration was tested with the Langmuir, Freundlich, Tempkin and Dubinin–Radushkevich (D–R) isotherm equations. Linear regression is frequently used to determine the best-fitting isotherm, and the applicability of isotherm equations is compared by judging the correlation coefficients.

3.4.1. Langmuir isotherm

The theoretical Langmuir isotherm [26] is valid for sorption of a solute from a liquid solution as monolayer adsorption on a surface containing a finite number of identical sites. Langmuir isotherm model assumes uniform energies of adsorption onto the surface without transmigration of adsorbate in the plane of the surface [27]. Therefore, the Langmuir isotherm model was chosen for estimation of the maximum adsorption capacity corresponding to complete monolayer coverage on the sorbent surface. The Langmuir nonlinear equation is commonly expressed as followed:

$$q_e = \frac{Q_m K_a C_e}{1 + K_a C_e} \quad (2)$$

In Eq. (2), C_e and q_e are as defined before in Eq. (1), Q_m is a constant reflect a complete monolayer (mg g^{-1}); K_a is adsorption equilibrium constant (L mg^{-1}) that is related to the apparent energy of sorption. The Langmuir isotherm Eq. (2) can be linearized into the following form [28,29].

Table 1
Comparison of the coefficients isotherm parameters for DB-86 adsorption onto COP

Isotherm model	Orange peel activated carbon concentrations (g L^{-1})		
	2	4	6
Langmuir			
Q_m (mg g^{-1})	33.78	30.58	20.16
K_a (L mg^{-1})	0.12	0.07	0.35
No. of parameter estimated	2	2	2
Data point available	4	4	5
R^2	0.990	0.987	0.988
Freundlich			
$1/n$	0.382	0.522	0.257
K_F (mg g^{-1})	7.13	3.42	8.07
No. of parameter estimated	2	2	2
Data point available	4	5	5
R^2	0.983	0.987	0.989
Redlich–Peterson			
A (L g^{-1})	20.0	50.0	100.0
B (L $mg^{-1})^g$	2.61	18.97	12.02
g	0.609	0.398	0.740
No. of parameter estimated	3	3	3
Data point available	4	5	5
R^2	0.945	0.962	0.969
Tempkin			
α (L g^{-1})	1.42	0.96	6.99
β (mg L^{-1})	6.96	6.26	3.64
b	355.9	395.8	680.8
No. of parameter estimated	2	2	2
Data point available	4	5	3
R^2	0.991	0.995	1.000
Dubinin–Radushkevich			
Q_m (mg g^{-1})	29.43	21.96	18.25
K ($\times 10^6$ mol^2 kJ^{-2})	2.30	2.60	2.50
E (kJ mol^{-1})	0.466	0.468	0.472
No. of parameter estimated	2	2	2
Data point available	3	5	5
R^2	1.000	0.996	0.998

Langmuir-1

$$\frac{C_e}{q_e} = \frac{1}{K_a Q_m} + \frac{1}{Q_m} \times C_e \quad (3)$$

A plot of C_e/q_e versus C_e should indicate a straight line of slope $1/Q_m$ and an intercept of $1/(K_a Q_m)$.

The results obtained from the Langmuir model for the removal of DB-86 onto COP are shown in Table 1. The correlation coefficients reported in Table 1 showed strong positive evidence on the adsorption of DB-86 onto COP follows the Langmuir isotherm. The applicability of the four linear forms of Langmuir model to COP was proved by the high correlation coefficients $R^2 > 0.99$. This suggests that the Langmuir isotherm provides a good model of the sorption system. The maximum monolayer capacity Q_m obtained from the Langmuir is 33.78 mg g^{-1}. Unmodified orange peel was previously used to remove different dyes from aqueous solution [17–21] and the maximum capacity of dyes removal was reported in Table 2. The Q_m (33.78 mg g^{-1}) obtained for activated carbon developed from orange peel is higher than that obtained for untreated orange peel.

3.4.2. The Freundlich isotherm

The Freundlich isotherm model [30] is the earliest known equation describing the adsorption process. It is an empirical equation can be used for non-ideal sorption that involves heterogeneous sorption. The Freundlich isotherm can be derived assuming a logarithmic decrease in the enthalpy of sorption with the increase in the fraction of occupied sites and is commonly given by the following

Table 2
Reported maximum dyes adsorption obtained for orange peel

Dye name	Maximum adsorption (mg L^{-1})	Reference
Methyl orange	20.5	[17]
Methylene blue	18.6	[17]
Rhodamine B	14.3, 3.23	([17,18] respectively)
Congo red	14.0, 22.4	([17,18] respectively)
Methyl violet	11.5	[17]
Amido black	7.9	[17]
Acid violet 17	19.88	[17,19]
Direct red 23	10.72	[20,21]
Direct red 80	21.05	[20,21]

non-linear equation:

$$q_e = K_F C_e^{1/n} \quad (4)$$

where K_F is a constant for the system, related to the bonding energy. K_F can be defined as the adsorption or distribution coefficient and represents the quantity of dye adsorbed onto adsorbent for unit equilibrium concentration. $1/n$ is indicating the adsorption intensity of dye onto the sorbent or surface heterogeneity, becoming more heterogeneous as its value gets closer to zero. A value for $1/n$ below 1 indicates a normal Langmuir isotherm while $1/n$ above 1 is indicative of cooperative adsorption. Eq. (4) can be linearized in the logarithmic form (Eq. (5)) and the Freundlich constants can be determined:

$$\log q_e = \log K_F + \frac{1}{n}\log C_e \quad (5)$$

The applicability of the Freundlich sorption isotherm was also analyzed, using the same set of experimental data, by plotting $\log(q_e)$ versus $\log(C_e)$. The data obtained from linear Freundlich isotherm plot for the adsorption of the DB-86 onto COP is presented in Table 1. The correlation coefficients (>0.98) showed that the Freundlich model is comparable to the Langmuir model. The $1/n$ is lower than 1.0, indicating that DB-86 is favorably adsorbed by COP.

3.4.3. The Redlich–Peterson isotherm

The Redlich–Peterson isotherm [31] contains three constants, A, B and g, and involves the features of both the Langmuir and the Freundlich isotherm models. It can be described by the following non-linear equation (6):

$$q_e = \frac{AC_e}{1 + BC_e^g} \quad (6)$$

where g must fluctuated between 0 and 1 and it can characterize the isotherm as if $g = 1$, the Langmuir will be the preferable isotherm, while if $g = 0$, the Freundlich will be the preferable isotherm. The three isotherm constants A, B and g, can be evaluated from Eq. (6) using nonlinear regression analysis in SPSS program Version 10.0, which is applicable to computer operation was developed to calculate the isotherm constants through maximization of the coefficient of determination and the results were included in Table 1. The coefficient R^2 for Redlich–Peterson isotherm was lower than it for Langmuir and Freundlich isotherm models for data obtained from adsorption of DB-86 onto COP.

3.4.4. The Tempkin isotherm

Tempkin adsorption isotherm model was used to evaluate the adsorption potentials of the COP for DB-86. The derivation of the Tempkin isotherm assumes that the fall in the heat of sorption is linear rather than logarithmic, as implied in the Freundlich equation. The Tempkin isotherm has commonly been applied in the following form [32–34]:

$$q_e = \frac{RT}{b}\ln(AC_e) \quad (7)$$

The Tempkin isotherm Eq. (7) can be simplified to the following equation:

$$q_e = \beta \ln \alpha + \beta \ln C_e \quad (8)$$

where $\beta = (RT)/b$, T is the absolute temperature in Kelvin and R is the universal gas constant, 8.314 J (mol K)$^{-1}$. The constant b is related to the heat of adsorption [35,36]. The adsorption data were analyzed according to the linear form of the Tempkin isotherm equation (8). Examination of the data shows that the Tempkin isotherm fitted well the DB-86 adsorption data for COP. The linear isotherm constants and coefficients of determination are presented in Table 1. The heat of DB-86 adsorption onto COP was found to increase from 0.356 to 0.681 kJ mol^{-1} with increase of COP dose from 2.0 to 6.0 g L^{-1}. The correlation coefficients R^2 obtained from Tempkin model were comparable to that obtained for Langmuir and Freundlich equations, which explain the applicability of Tempkin model to the adsorption of DB-86 onto COP.

3.4.5. The Dubinin–Radushkevich (D–R) isotherm

The D–R model was also applied to estimate the porosity apparent free energy and the characteristics of adsorption [37–39]. The D–R isotherm dose not assumes a homogeneous surface or constant sorption potential. The D–R model has commonly been applied in the following Eq. (9) and its linear form can be shown in Eq. (10):

$$q_e = Q_m \exp(-K\varepsilon^2) \quad (9)$$

$$\ln q_e = \ln Q_m - K\varepsilon^2 \quad (10)$$

where K is a constant related to the adsorption energy, Q_m the theoretical saturation capacity, ε the Polanyi potential, calculated from Eq. (11).

$$\varepsilon = RT \ln\left(1 + \frac{1}{C_e}\right) \quad (11)$$

The slope of the plot of $\ln q_e$ versus ε^2 gives K (mol^2 (kJ^2)$^{-1}$) and the intercept yields the adsorption capacity, Q_m (mg g^{-1}). The mean free energy of adsorption (E), defined as the free energy change when one mole of ion is transferred from infinity in solution to the surface of the solid, was calculated from the K value using the following relation [40]:

$$E = \frac{1}{\sqrt{2K}} \quad (12)$$

The calculated value of D–R parameters is given in Table 1. The saturation adsorption capacity Q_m obtained using D–R isotherm model for adsorption of DB-86 onto COP is 29.43 mg g^{-1} at 2.0 g L^{-1} sorbent dose, which is close to that obtained (33.78 mg g^{-1}) from Langmuir isotherm model (Table 1). However, the Q_m calculated from D–R and Langmuir isotherm models at higher dose of activated carbon COP (6.0 g L^{-1}) were very close to each other. The values of E calculated using Eq. (12) are 0.466–0.472 kJ mol^{-1}, which indicating that the physico-sorption process play the significant role in the adsorption of DB-86 onto COP.

3.5. Kinetic models applied to the adsorption of DB-86 onto COP

Several steps can be used to examine the controlling mechanism of sorption process such as chemical reaction, diffusion control and mass transfer; kinetic models are used to test experimental data from the adsorption of DB-86 onto COP. The kinetics of DB-86 adsorption onto COP is required for selecting optimum operating

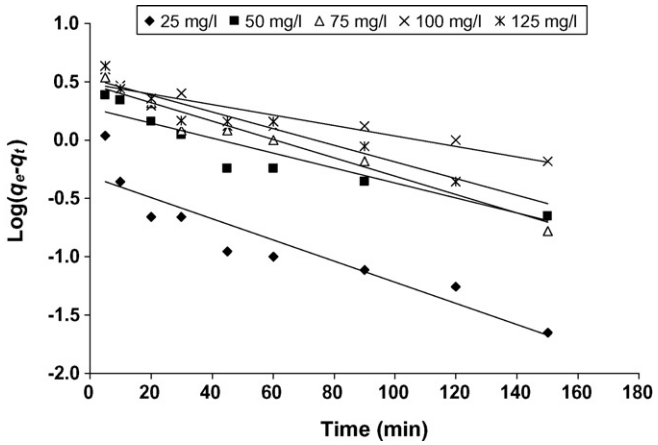

Fig. 5. Pseudo-first-order kinetics for DB-86 adsorption onto COP. Conditions: adsorbent dosage 6 g L^{-1}, pH 2.0, temperature 25 ± 2 °C.

conditions for the full-scale batch process. The kinetic parameters, which are helpful for the prediction of adsorption rate, give important information for designing and modeling the adsorption processes. Thus, the kinetics of DB-86 adsorption onto COP were analyzed using pseudo-first-order [41], pseudo-second-order [42], Elovich [43–45] and intraparticle diffusion [46,47] kinetic models. The conformity between experimental data and the model-predicted values was expressed by the correlation coefficients (R^2, values close or equal to 1). The relatively higher value is the more applicable model to the kinetics of DB-86 adsorption onto COP.

3.5.1. Pseudo-first-order equation

The adsorption kinetic data were described by the Lagergren pseudo-first-order model [41], which is the earliest known equation describing the adsorption rate based on the adsorption capacity. The differential equation is generally expresses a follows:

$$\frac{dq_t}{dt} = k_1(q_e - q_t) \tag{13}$$

where q_e and q_t are the adsorption capacity at equilibrium and at time t, respectively (mg g^{-1}), k_1 is the rate constant of pseudo-first-order adsorption (L min^{-1}). Integrating Eq. (13) for the boundary conditions $t = 0$–t and $q_t = 0$–q_t gives

$$\log\left(\frac{q_e}{q_e - q_t}\right) = \frac{k_1}{2.303}t \tag{14}$$

Eq. (14) can be rearranged to obtain the following linear form:

$$\log(q_e - q_t) = \log(q_e) - \frac{k_1}{2.303}t \tag{15}$$

In order to obtain the rate constants, the values of $\log(q_e - q_t)$ were linearly correlated with t by plot of $\log(q_e - q_t)$ versus t to give a linear relationship from which k_1 and predicted q_e can be determined from the slope and intercept of the plot, respectively (Fig. 5). The variation in rate should be proportional to the first power of concentration for strict surface adsorption. However, the relationship between initial solute concentration and rate of adsorption will not be linear when pore diffusion limits the adsorption process. Fig. 5 shows that the pseudo-first-order equation fits well for the first 30 min and thereafter the data deviate from theory. Thus, the model represents the initial stages where rapid adsorption occurs well but cannot be applied for the entire adsorption process. Furthermore, the experimental q_e values do not agree with the calculated ones, obtained from the linear plots and the correlation coefficient R^2 are relatively low for most adsorption data (Table 3). This shows that the adsorption of DB-86 onto COP cannot be applied and the reaction mechanism is not a first-order reaction.

3.5.2. Pseudo-second-order equation

The adsorption kinetic may be described by the pseudo-second-order model [42]. The differential equation is generally given as follows:

$$\frac{dq_t}{dt} = k_2(q_e - q_t)^2 \tag{16}$$

where k_2 (g(mg min)$^{-1}$) is the second-order rate constant of adsorption. Integrating Eq. (16) for the boundary conditions $q_t = 0$–q_t at $t = 0$–t is simplified as can be rearranged and linearized to obtain:

$$\left(\frac{t}{q_t}\right) = \frac{1}{k_2 q_e^2} + \frac{1}{q_e}(t) \tag{17}$$

The second-order rate constants were used to calculate the initial sorption rate, given by the following equation:

$$h = k_2 q_e^2 \tag{18}$$

Table 3
Comparison of the first- and second-order adsorption rate constants and calculated and experimental q_e values for different initial DB-86 and COP

Parameter			First-order kinetic model			Second-order kinetic model			
COP concentration (g L^{-1})	DB-86 (mg L^{-1})	q_e (experimental)	k_1	q_e (calculated)	R^2	k_2	q_e (calculated)	h	R^2
2	25	10.84	0.01	3.51	0.650	0.012	10.73	1.36	0.994
	50	19.44	0.02	8.79	0.931	0.005	20.04	2.03	0.994
	75	24.26	0.03	9.65	0.930	0.006	25.00	3.58	0.996
	100	29.14	0.01	7.61	0.914	0.006	29.41	5.03	0.997
	125	37.33	0.02	8.78	0.838	0.007	37.59	9.35	0.998
4	25	6.17	0.03	1.71	0.960	0.043	6.31	1.71	1.000
	50	10.02	0.02	3.16	0.854	0.016	10.16	1.70	0.996
	75	13.78	0.01	3.6	0.726	0.034	13.99	6.56	1.000
	100	18.71	0.01	5.53	0.903	0.007	17.99	2.41	0.988
	125	22.64	0.01	5.41	0.832	0.008	21.98	3.92	0.993
6	25	4.17	0.02	0.49	0.858	0.144	4.19	2.53	1.000
	50	8.11	0.01	1.89	0.868	0.029	8.15	1.91	0.999
	75	11.62	0.02	3.02	0.957	0.019	11.75	2.63	0.999
	100	15.12	0.01	5.53	0.850	0.016	14.99	3.63	0.998
	125	17.74	0.02	3.38	0.919	0.016	17.95	5.15	0.999

k_1 (min^{-1}), k_2 (g(mg min)$^{-1}$), q_e (mg g^{-1}), h (mg(g min)$^{-1}$).

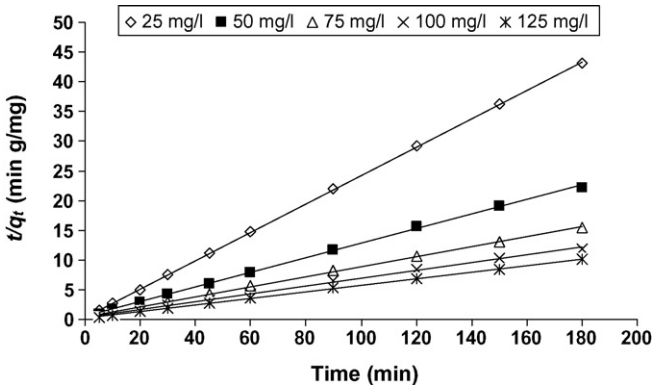

Fig. 6. Plot of the pseudo-second-order model at different initial DB-86 concentrations, COP 6 g L^{-1}, pH 2.0, temperature 25 ± 2 °C.

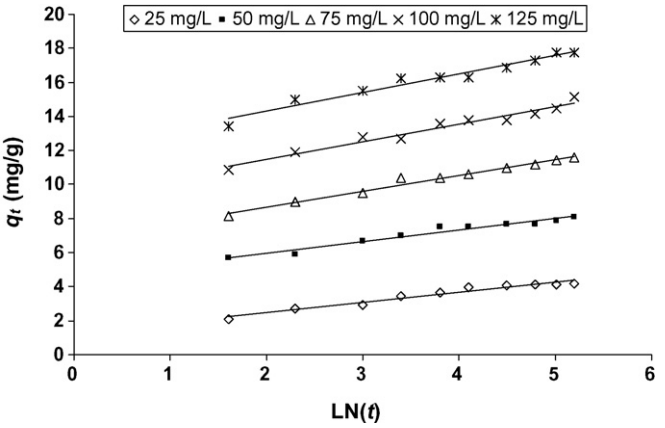

Fig. 7. Elovich model plot for the adsorption of DB-86 onto COP (6.0 g L^{-1}) at different initial dye concentrations (25, 50, 75, 100 and 125 mg L^{-1}).

If the second-order kinetics is applicable, then the plot of t/q_t versus t should show a linear relationship. Values of k_2 and equilibrium adsorption capacity q_e were calculated from the intercept and slope of the plots of t/q_t versus t (Fig. 6). The linear plots of t/q_t versus t show good agreement between experimental and calculated q_e values at different initial DB-86 and adsorbent concentrations (Table 3). The correlation coefficients for the second-order kinetic model are greater than 0.993, which led to believe that the pseudo-second-order kinetic model provided good correlation for the biosorption of different initial of DB-86 onto COP.

The values of initial sorption (h) that represents the rate of initial sorption, is practically increased from 1.36 to 9.35, 1.70 to 3.92, and 1.91 to 5.15 mg (g min)$^{-1}$ with the increase in initial DB-86 concentrations from 25 to 125 mg L^{-1} onto COP dose 2.0, 4.0 and 5.0 g L^{-1}, respectively (Table 3). It was observed that the pseudo-second-order rate constant (k_2) decreased from 0.012 to 0.007, 0.043 to 0.008 and 0.144 to 0.016 with increased initial DB-86 concentration from 25 to 125 mg L^{-1} for COP doses of 2, 4 and 6 g L^{-1}, respectively.

3.5.3. Elovich equation

The Elovich equation is another rate equation based on the adsorption capacity generally expressed as following [43–45]:

$$\frac{dq_t}{dt} = B_E \exp(-A_E q_t) \quad (19)$$

where B_E is the initial adsorption rate (mg (g min)$^{-1}$) and A_E is the de-sorption constant (g mg^{-1}) during any experiment.

It is simplified by assuming $A_E B_E t \gg t$ and by applying the boundary conditions $q_t = 0$ at $t = 0$ and $q_t = q_t$ at $t = t$ Eq. (19) becomes:

$$q_t = \frac{1}{A_E}\ln(B_E A_E) + \frac{1}{A_E}\ln(t) \quad (20)$$

If DB-86 adsorption by COP fits the Elovich model, a plot of q_t versus ln(t) should yield a linear relationship with a slope of ($1/A_E$) and an intercept of ($1/A_E$) ln($A_E B_E$) (Fig. 7). Thus, the constants can be obtained from the slope and the intercept of the straight line (Table 4). The initial adsorption rate B_E increase from 4 to 508, 1186 to 92,299 and 5 to 69,005 mg (g min)$^{-1}$ with increase of initial DB-86 concentration from 25 to 125 mg L^{-1} on COP dose of 2, 4 and 6 g L^{-1}, respectively. Similar pattern is mentioned above for the initial adsorption rate, h, obtained from pseudo-second-order model. The desorption constant, A_E, decrease from 0.55 to 0.27, 2.04 to 0.78 and 1.69 to 0.91 g mg^{-1} with increase in the initial DB-86 concentration from 25 to 125 mg L^{-1} over COP dose of 2, 4 and 6 g L^{-1}, respectively (Table 4).

3.5.4. The intraparticle diffusion model

The adsorbate species are most probably transported from the bulk of the solution into the solid phase through intraparticle dif-

Table 4
The parameters obtained from Elovich kinetics model and intraparticle diffusion model using different initial DB-86 concentrations.

COP concentration (g L^{-1})	DB-86 concentration (mg L^{-1})	Elovich			Intraparticle diffusion		
		A_E	B_E	R^2	K_{dif}	C	R^2
2.0	25	0.55	4	0.977	0.13	8.23	0.993
	50	0.37	17	0.989	0.62	11.26	0.992
	75	0.33	60	0.970	0.75	16.04	0.988
	100	0.31	141	0.986	0.65	20.42	0.992
	125	0.27	508	0.992	0.50	30.10	0.972
4.0	25	2.04	1186	0.937	0.04	5.72	0.971
	50	1.20	751	0.962	0.18	7.65	0.993
	75	0.90	3716	0.964	0.20	11.99	0.977
	100	0.87	11049	0.963	0.28	13.10	0.983
	125	0.78	92299	0.991	0.30	16.96	0.995
6.0	25	1.69	5	0.955	0.02	3.94	0.979
	50	1.46	561	0.957	0.07	7.00	0.976
	75	1.07	1368	0.980	0.18	9.21	0.998
	100	0.96	8449	0.962	0.28	11.08	0.997
	125	0.91	69005	0.960	0.29	14.09	0.997

A_E (g mg^{-1}), B_E (mg (g min)$^{-1}$), K_{dif} (mg g^{-1} $min^{-1/2}$) and C (mg g^{-1}).

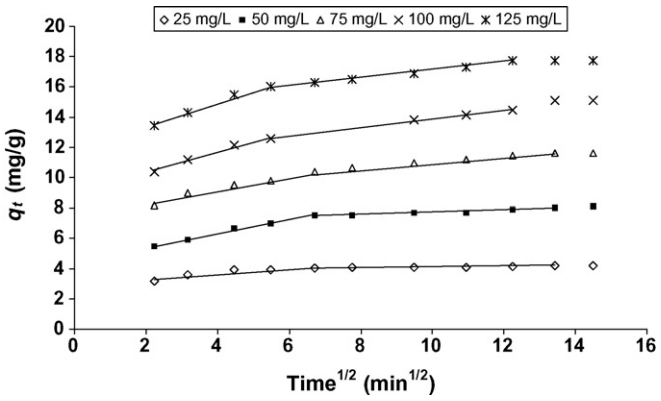

Fig. 8. Intraparticle diffusion model plot for the adsorption of DB-86 onto COP (6.0 g L^{-1}) at different initial dye concentration (25, 50, 75, 100 and 125 mg L^{-1}) and room temperature.

fusion/transport process, which is often the rate-limiting step in many adsorption processes, especially in a rapidly stirred batch reactor [48]. Since the DB-86 are probably transported from its aqueous solution to the COP by intraparticle diffusion, so the intraparticle diffusion is another kinetic model should be used to study the rate of DB-86 adsorption onto COP. The possibility of intraparticular diffusion was explored by using the intraparticle diffusion model, which is commonly expressed by the following equation:

$$q_t = K_{dif} t^{1/2} + C \quad (21)$$

where C (mg g^{-1}) is the intercept and K_{dif} is the intraparticle diffusion rate constant (in mg g^{-1} $min^{-1/2}$). The values of q_t were found to be linearly correlated with values of $t^{1/2}$ (Fig. 8) and the rate constant K_{dif} directly evaluated from the slope of the regression line (Table 4). The values of intercept C (Table 4) provide information about the thickness of the boundary layer, the resistance to the external mass transfer increase as the intercept increase. The constant C was found to increase from 8.23 to 30.10 with increase of dye concentration from 25 to 125 mg L^{-1}, which indicating the increase of the thickness of the boundary layer and decrease of the chance of the external mass transfer and hence increase of the chance of internal mass transfer. On the other hand, the constant C was found to decrease with the increase of COP dose from 2.0 to 6.0 g L^{-1}, which reflect decrease of the thickness of the boundary layer and hence increase of the chance of the external mass transfer. The R^2 values given in Table 4 are close to unity indicating the application of this model. This may confirm that the rate-limiting step is the intraparticle diffusion process. The intraparticle diffusion rate constant, K_{dif}, were in the range of 0.13–0.50 mg g^{-1} $min^{-1/2}$ and it decrease with increase of initial dye concentration and increase of COP dose. The linearity of the plots demonstrated that intraparticle diffusion played a significant role in the uptake of the adsorbate by sorbent. However, Fig. 8 shows two trend lines for all studied initial DB-86 concentrations over COP, which confirms that adsorption of the chromium onto the COP is independent of one another, as plot usually shows two intersecting lines depending on the exact mechanism, the first one of these lines representing surface adsorption at the beginning of the reaction and the second one is the intraparticle diffusion at the end of the reaction. As still there is no sufficient indication about which of the two steps was the rate-limiting step. Ho [49] has shown that if the intraparticle diffusion is the sole rate-limiting step, it is essential for the q_t versus $t^{1/2}$ plots to pass through the origin, which is not the case in Fig. 8, it may be concluded that surface adsorption and intraparticle diffusion were concurrently operating during the DB-86 and COP interactions.

4. Conclusion

The results of this investigation show that activated carbon developed from orange peel has a suitable adsorption capacity for the removal of DB-86 from aqueous solutions. The equilibrium adsorption is practically achieved in 180 min. The experimental results were analyzed by using Langmuir, Freundlich, Redlich–Peterson, Tempkin and Dubinin–Radushkevich isotherm models and the correlation coefficients for Langmuir, Tempkin and Dubinin–Radushkevich equation fitted better than Freundlich and Redlich–Peterson equations. Adsorption behavior is described by a monolayer Langmuir-type isotherm. The kinetic study of DB-86 on COP was performed based on pseudo-first-order, pseudo-second-order, Elovich and intraparticle diffusion equations. The data indicate that the adsorption kinetics follow the pseudo-second-order rate with intraparticle diffusion as one of the rate determining steps. The present study concludes that the COP could be employed as low-cost adsorbents as alternatives to commercial activated carbon for the removal of color and dyes from water and wastewater, in general and for the removal of DB-86 in particular.

References

[1] P. Grau, Textile industry wastewaters treatment, Water Sci. Technol. 24 (1991) 97.
[2] M.F. Boeniger, Carcinogenity of Azo Dyes Derived from Benzidine, Department of Health and Human Services (NIOSH), Cincinnati, OH, 1980, Pub. No. 8-119.
[3] Kirk-Othomer, Encyclope Chemical Technology, 8th ed., 1994, pp. 547–672.
[4] V.A. Shenai, Azo dyes on textiles vs German ban: an objective assessment. Part III. Another study, Colourage XLIII (8) (1996) 41.
[5] J.C. Greene, G.L. Baughman, Effects of 46 dyes on population growth of fresh green algae *Selenastrum capricornutum*, Textile Chemist Colorist 28 (4) (1996) 23.
[6] C. Saha, Eco-textile: a novel concept of cleaner product, Textile Dyer Printer XXIX (21) (1996) 13.
[7] D.A.S. Phillips, Environmentally friendly, productive and reliable priorities for cotton dyes and dyeing processes, J. Soc. Dyers Colorists 112 (1996) 183.
[8] K.R. Ramakrishna, T. Viraraghavan, Dye removal using low cost adsorbent, Water Sci. Technol. 36 (1997) 189–196.
[9] A. Bozdogan, H. Goknil, The removal of the color of textile dyes in wastewater by the use of recycled coagulant, MU Fen. Billimeri. Dergisi. Sayi. 4 (1987) 83.
[10] K. Majewska-Nowak, Effect of flow conditions on ultra-filtration efficiency of dye solutions and textile effluents, Desalination 71 (1989) 127.
[11] O.R. Shendrik, Electro membrane removal of organic dyes from wastewaters, Kimiyi. Technol. Vody. 11 (1989) 467.
[12] Z. Ding, C.W. Min, W.Q. Hui, A study on the use of bipolar particles-electrode in the decolorization of dying effluents and its principle, Water Sci. Technol. 19 (3/4) (1987) 39.
[13] O. Abdelwahab, A. El Nemr, A. El-Sikaily, A. Khaled, Biosorption of Direct Yellow 12 from aqueous solution by marine green algae *Ulva Lactuca*, Chem. Ecol. 22 (2006) 253–266.
[14] A. El-Sikaily, A. Khaled, A. El Nemr, O. Abdelwahab, Removal of methylene blue from aqueous solution by marine green alga *Ulva lactuca*, Chem. Ecol. 22 (2006) 149–157.
[15] P. Cooper, Color in Dye House Effluent Soc Dyers and Colorists, Alden Press, Oxford, 1995.
[16] B. Shi, G. Li, D. Wang, C. Feng, H. Tang, Removal of direct dyes by coagulation: the performance of preformed polymeric aluminum species, J. Hazard. Mater. B 143 (2007) 567–574.
[17] G. Annadurai, R.-S. Juang, D.-J. Lee, Use of cellulose-based wastes for adsorption of dyes from aqueous solutions, J. Hazard. Mater. B 92 (2002) 263–274.
[18] C. Namasivayam, N. Muniasamy, K. Gayathri, M. Rani, K. Ranganathan, Removal of dyes from aqueous solutions by cellulosic waste orange peel, Bioresour. Technol. 57 (1996) 37–43.
[19] R. Sivaraj, C. Namasivayam, K. Kadirvelu, Orange peel as an adsorbent in the removal of Acid violet 17 (acid dye) from aqueous solutions, Waste Manage. 21 (2001) 105–110.
[20] M. Arami, N.Y. Limaee, N.M. Mahmoodi, N.S. Tabrizi, Removal of dyes from colored textile wastewater by orange peel adsorbent: equilibrium and kinetic studies, J. Colloid Interf. Sci. 288 (2005) 371–376.
[21] F. Doulati Ardejani, Kh. Badii, N. Yousefi Limaee, N.M. Mahmoodi, M. Arami, S.Z. Shafaei, A.R. Mirhabibi, Numerical modeling and laboratory studies on the removal of Direct Red 23 and Direct Red 80 dyes from textile effluents using orange peel, a low-coast adsorbent, Dyes Pigments 73 (2007) 178–185.
[22] A. El Nemr, A. El Sikaily, O. Abdelwahab, A. Khaled, Direct Dye (DB-86) removal from aqueous solution by adsorption using activated carbon from orange peel, in: Proceedings of the International Conference on Aquatic Resources:

Needs and Benefits NIOF, Alexandria, Egypt, September 18–21st, 2006, p. 86.
[23] C. Namasivayam, D. Kavitha, Removal of Congo Red from water by adsorption onto activated carbon prepared from coir pith, an agricultural solid waste, Dyes Pigments 54 (1) (2002) 47–58.
[24] C. Namasivayam, R. Radhika, S. Suba, Uptake of dyes by promising locally available agricultural solid wastes coir pith, Waste Manage. 21 (4) (2001) 381–387.
[25] P.K. Malik, Dye removal from wastewater using activated carbon developed from sawdust: adsorption equilibrium and kinetics, J. Hazard. Mater. B 113 (2004) 81–88.
[26] I. Langmuir, The constitution and fundamental properties of solids and liquids, J. Am. Chem. Soc. 38 (1916) 2221–2295.
[27] M. Doğan, M. Alkan, Y. Onganer, Adsorption of methylene blue from aqueous solution onto perlite, Water Air Soil Pollut. 120 (2000) 229–249.
[28] D.G. Kinniburgh, General purpose adsorption isotherms, Environ. Sci. Technol. 20 (1986) 895–904.
[29] E. Longhinotti, F. Pozza, L. Furlan, M.D.N.D. Sanchez, M. Klug, M.C.M. Laranjeira, V.T. Favere, Adsorption of anionic dyes on the biopolymer chitin, J. Brazil. Chem. Soc. 9 (1998) 435–440.
[30] H.M.F. Freundlich, Über die adsorption in lösungen, Z. Phys. Chem. (Leipzig) 57A (1906) 385–470.
[31] O. Redlich, D.L. Peterson, A useful adsorption isotherm, J. Phys. Chem. 63 (1959) 1024.
[32] C. Aharoni, D.L. Sparks, Kinetics of soil chemical reactions—a theoretical treatment, in: D.L. Sparks, D.L. Suarez (Eds.), Rate of Soil Chemical Processes, Soil Science Society of America, Madison, WI, 1991, pp. 1–18.
[33] C. Aharoni, M. Ungarish, Kinetics of activated chemisorption. Part 2. Theoretical models, J. Chem. Soc., Faraday Trans. 73 (1977) 456–464.
[34] X.S. Wang, Y. Qin, Equilibrium sorption isotherms for of Cu^{2+} on rice bran, Process Biochem. 40 (2005) 677–680.
[35] G. Akkaya, A. Ozer, Adsorption of acid red 274 (AR 274) on *Dicranella varia*: determination of equilibrium and kinetic model parameters, Process Biochem. 40 (11) (2005) 3559–3568.
[36] C.I. Pearce, J.R. Lioyd, J.T. Guthrie, The removal of color from textile wastewater using whole bacterial cells: a review, Dyes Pigments 58 (2003) 179–196.
[37] M.M. Dubinin, The potential theory of adsorption of gases and vapors for adsorbents with energetically non-uniform surface, Chem. Rev. 60 (1960) 235–266.
[38] M.M. Dubinin, Modern state of the theory of volume filling of micropore adsorbents during adsorption of gases and steams on carbon adsorbents, Zhurnal Fizicheskoi Khimii 39 (1965) 1305–1317.
[39] L.V. Radushkevich, Potential theory of sorption and structure of carbons, Zhurnal Fizicheskoi Khimii 23 (1949) 1410–1420.
[40] S. Kundu, A.K. Gupta, Investigation on the adsorption efficiency of iron oxide coated cement (IOCC) towards As(V)—kinetics, equilibrium and thermodynamic studies, Colloid Surf. A: Physicochem. Eng. Aspects 273 (2006) 121–128.
[41] S. Lagergren, Zur theorie der sogenannten adsorption geloster stoffe Kungliga Svenska Vetenskapsakademiens, Handlingar 24 (1898) 1–39.
[42] Y.S. Ho, G. McKay, D.A.J. Wase, C.F. Foster, Study of the sorption of divalent metal ions on to peat, Adsorp. Sci. Technol. 18 (2000) 639–650.
[43] S.H. Chien, W.R. Clayton, Application of Elovich equation to the kinetics of phosphate release and sorption on soils, Soil Sci. Soc. Am. J. 44 (1980) 265–268.
[44] D.L. Sparks, Kinetics of Reaction in Pure and Mixed Systems, in Soil Physical Chemistry, CRC Press, Boca Raton, 1986.
[45] J. Zeldowitsch, Über den mechanismus der katalytischen oxidation von CO an MnO_2, Acta Physicochim. URSS 1 (1934) 364–449.
[46] W.J. Weber, J.C. Morris, Kinetics of adsorption on carbon from solution, J. Sanity Eng. Div. Am. Soc. Civil Eng. 89 (1963) 31–59.
[47] K. Srinivasan, N. Balasubramanian, T.V. Ramakrishan, Studies on chromium removal by rice husk carbon, Indian J. Environ. Health 30 (1988) 376–387.
[48] G. McKay, The adsorption of dyestuff from aqueous solution using activated carbon: analytical solution for batch adsorption based on external mass transfer and pore diffusion, Chem. Eng. J. 27 (1983) 187–195.
[49] Y.S. Ho, Removal of copper ions from aqueous solution by tree fern, Water Res. 37 (2003) 2323–2330.